Hindawi
Journal of Nanotechnology
Volume 2022, Article ID 5816063, 9 pages
https://doi.org/10.1155/2022/5816063

Research Article

Bio-Inspired C/N/TiO_2 Hybrid Composite Heterostructure: Enhanced Photocatalytic Activity under Visible Light

Shyam Sundar Gandi,[1] **Suman Gandi**,[2] **Saidi Reddy Parne**,[2] **Motilal Lakavat**,[3] **Nageswara Rao Lakkimsetty**,[3] **and Gangaraju Gedda**[4]

[1]*Department of Science and Humanities, Sumathi Reddy Institute of Technology for Women, Warangal, Telangana 506371, India*
[2]*Department of Applied Sciences, National Institute of Technology Goa, Ponda 403401, India*
[3]*College of Engineering, National University of Science & Technology, P. O. Box 620, Seeb PC 130, Oman*
[4]*Department of Chemistry, School of Engineering, Presidency University, Bangalore, Karnataka 560064, India*

Correspondence should be addressed to Shyam Sundar Gandi; g_shyamsundar@sritw.org and Gangaraju Gedda; gangaraju.g@vishnu.edu.in

Received 19 April 2022; Revised 12 July 2022; Accepted 15 July 2022; Published 16 September 2022

Academic Editor: Brajesh Kumar

The hydrothermal treatment was used to create a natural hierarchical bio-inspired carbon and nitrogen-doped C/N/TiO_2 hybrid composite. It is the goal of this work to investigate the photocatalytic activity of bio-inspired C/N/TiO_2 hybrid composite. Techniques such as X-ray powder diffraction, scanning electron microscopy, UV-Vis absorption spectroscopy, *FTIR*, Raman, and photoluminescence spectroscopy were used to explore the structural, morphological, and photocatalysis characteristics of the bio-inspired C/N/TiO_2 hybrid composite. By doping carbon and nitrogen, TiO_2 nanotubes were able to improve the photocatalyst properties of the C/N/TiO_2 hybrid composite, decrease the energy band gap (~2.55 eV), and result in increased electron transfer efficiency when compared to pure TiO_2. The photocatalytic degradation of pollutants (rhodamine B (RhB)) is made possible by the use of a bio-inspired C/N/TiO_2 hybrid composite that has high interconnectivity and an easily accessible surface.

1. Introduction

In recent years, photocatalysis has become increasingly popular in the development of energy-efficient, ecologically beneficial, and long-lasting processes [1–6]. Despite the fact that other photo-catalyst candidates have been investigated, titanium dioxide (TiO_2) has been the most thoroughly investigated material, and it is now considered to be the most likely photocatalyst for industrial-scale applications due to its high photoactivity efficiency, long-term stability, nontoxicity, and low price [7–11]. Recent research on the use of TiO_2 as a photocatalyst has concentrated on enhancing the material's photocatalytic activity under visible light and increasing its specific surface area [12]. This is being done in an effort to boost the efficiency with which solar energy is converted while simultaneously bringing down the associated costs. However, the large bandgap (~3.2 eV) of TiO_2 restricts the photocatalytic activity in the ultraviolet wavelength range, which contributes less than 5% of the total energy of the overall solar spectrum [13–15]. It is also important to note that TiO_2 is limited by the rapid recombination of photo-generated electron-hole pairs, which is particularly noticeable in the absence of electron donors or acceptors, as it results in significant energy loss and an extremely small active photocatalytic reactive zone [15–17].

Numerous studies have sought to improve the photocatalytic activity of TiO_2 under visible light by doping it with metal/nonmetal anions [18–21]. In the case of metal ion doping, the photocatalytic activity failed due to insufficient interfacial electron transfer rates and charge carrier

recombination rates, which resulted in poor photocatalytic activity [19, 22, 23]. On the other hand, nonmetal anion doping often increases the specific surface area of TiO_2 photocatalysts, limits the growth of crystallite size, and increases the percentage of anatase phase in the photocatalyst [12, 19, 24, 25]. Additionally, nonmetal anions (C/N/P/S, etc.) can enhance the photocatalyst activity by moving its wavelength sensitivity from the ultraviolet to the visible-light area, which is made possible by the narrowing band gap of TiO_2 due to the presence of nonmetal anions [19, 26–30].

TiO_2 can be hydrogenated, doped with metals or nonmetals, combined with another semiconductor, or doped with nonmetals to enable it to be activated by visible light [1, 16, 19, 21, 31]. These are only a few of the many possible activation methods. It is also vital to the synthesis of TiO_2 photocatalysts in order to produce cost-effective, efficient photocatalysts. A number of different doping procedures, such as annealing, hydrothermal, microwave-assisted, and sol-gel techniques, have been examined [16, 18–20]. Each of these doping procedures has its own set of benefits and drawbacks, such as the amount of time required for preparation and the amount of photocatalytic activity that is achieved as a result. In the field of photocatalysis, numerous in-depth reviews and studies have been reported on the modification of TiO_2 to increase its sensitivity to visible light. Comparing the doping methods of non-metal-doped TiO_2 and the parameters impacts the synthesis and photocatalytic reactions.

Furthermore, two structural design strategies for increasing the photocatalytic activity of TiO_2 are being considered: monolithic three-dimensional (3D) nanostructuring and heterostructure with nonmetal anions such as carbon, nitrogen, phosphorus, and other carbon nanomaterials [18, 30, 32, 33]. A monolithic 3D nanostructure provides the most surface area possible in a given volume while also allowing for efficient reuse of the photocatalyst without the need for recollection. Heterostructuring with carbon nanomaterials aids in the efficient utilization of the solar spectrum and charge separation, as well as the production of TiO_2 photocatalysts with high efficiency [34, 35]. Therefore, it is critical to creating a simple, energy-efficient, and environmentally acceptable method for the synthesis of heterostructure carbon-based nanomaterials with high visible photocatalytic activity. Recently, bio-inspired carbon composites including TiO_2 nanoparticles have gained significant attention due to their ability to enhance the performance features of the individual components [36–38]. Moreover, when compared to bio-inspired synthesized nanomaterials, chemically synthesized nanomaterials rely on their efficiency in producing pure products while minimizing the number of preparation steps, without using either excessively harmful reagents or unstable precursors, and without generating particularly toxic by-products. In this work, we develop a bio-inspired approach for visible-light photocatalytic material, and urea as both carbon and nitrogen sources, and tannic acid was used as a carbon source as well as a reducing agent for the preparation of $C/N/TiO_2$ hybrid composite via hydrothermal treatment.

2. Experimental Section

The hydrothermal technique was employed to prepare the TiO_2 and $C/N/TiO_2$ hybrid composites as previously reported [39, 40], and the chemicals employed in this work were of analytical reagent grade (>99 percent purity) and acquired from SRL Chemicals, India. The following steps were taken in order to generate a bio-inspired $C/N/TiO_2$ hybrid composite: aqueous tannic acid solution ($40\,mg{\cdot}L^{-1}$) and 45 mL of deionized water were immersed in for 5 minutes with shaking after being added to the solution with 1 g of TiO_2 and 0.0445 g of urea. Following that, 20 mL MOPS (3-(N-Morpholino) propanesulfonic acid) solution (pH 7.4, $0.4\,mg{\cdot}L^{-1}$) was added to the solution and then transferred to a stainless autoclave lined with Teflon. The autoclave was kept at 160 degrees Celsius for 12 hours before being allowed to cool to ambient temperature with the air. The finished product was collected and carefully cleaned with water and ethanol before being dried in an oven at 80 degrees Celsius for 10 hours; then, the dried product was placed in an alumina boat and moved to a tube furnace with Ar gas flowing through it for 3 hours at 500 degrees Celsius (5 degrees per minute).

In order to analyze the samples, X-ray diffraction (XRD) analysis was carried out on them using a Philips PANalytical X-ray diffractometer, which operated between $2\theta = 20$ and 60° and had a sampling step of 0.05° and a counting duration of 2 seconds. A monochromatic Cu K_α radiation source was employed in this experiment, with a voltage of 40 kV and a current of 30 mA. The X'Pert HighScore Plus program was used to do both the quantitative analysis (weight percentages) and the phase determination of the samples. The morphology of the $C/N/TiO_2$ hybrid composite was studied using a scanning electron microscope (Zeiss GeminiSEM) operating at a 5 KeV accelerating voltage. The diffuse reflectance spectra of the materials were measured on a PerkinElmer Lambda 650 UV-Vis spectrophotometer in the ultraviolet-visible range. Fourier transformed infrared spectrophotometer (FTIR) carried out by using Bruker Optics, Germany (Model TENSOR 27, equipped with a KBr beam splitter), with an operating spectrum in the wavelength range between 4000 and 400 cm^{-1}. The carbon and nitrogen contents of the $C/N/TiO_2$ hybrid composite were determined using a TGA analysis (SII 6300 EXSTAR) system from Siemens. As a result of the photocatalytic dye degradation experiment, we measured the photodegradation of an RhB solution under xenon lamp (output power of 50 W) illumination to determine the rate of photodegradation of the solutions. A filter was utilized to select the range of the irradiated light, and only light with a wavelength of more than 400 nm was allowed to reach the sample. To summarize, 50.0 mg of sample and RhB solution ($50\,mg{\cdot}L^{-1}$) were used to assess the photocatalytic activity of the catalyst. For the first 20 minutes of the experiment, the mixture was magnetically agitated in the dark to bring the dye and catalyst into an adsorption-desorption equilibrium, and then, it was exposed to room temperature light irradiation. It was necessary to place the experimental solution in a quartz cuvette that was 100 mm distant from the light source. The

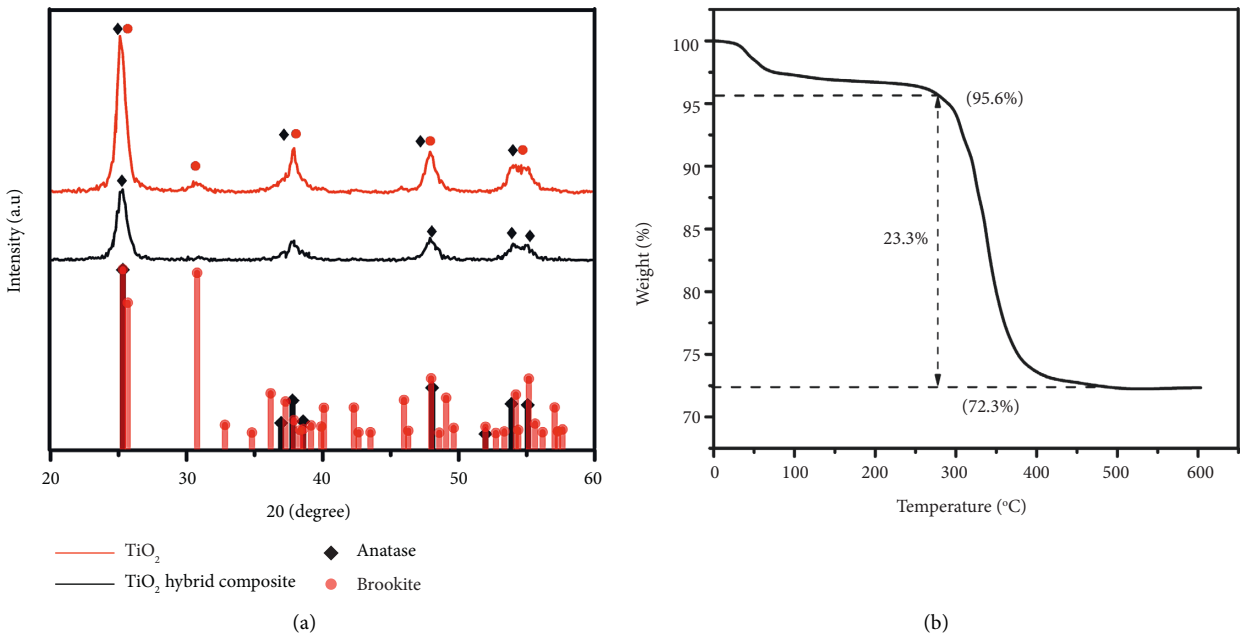

FIGURE 1: (a) XRD profiles of pure TiO_2 and bio-inspired C/N/TiO_2 hybrid composite. (b) Thermogravimetric analysis (TGA) of bio-inspired TiO_2 hybrid composite.

suspension was centrifuged to remove the scattered catalyst powder at regular intervals, with 5 mL of the suspension being removed at each interval. UV-Vis spectroscopy was used to evaluate the light absorption of the clear solutions at 553 nm (which corresponded to the absorbance of RhB).

3. Results and Discussion

As shown in Figure 1(a), the XRD profiles of pure TiO_2 and bio-inspired C/N/TiO_2 hybrid composites are well-indexed with the phase brookite (ICSD Reference code: 98-000-3869) and anatase (ICSD Reference code: 98-000-5224), and there are no further impurities in the samples. Pure TiO_2 has anatase (80%) and brookite (20%) phases composition, whereas bio-inspired C/N/TiO_2 hybrid composites have complete tetragonal anatase (100%) phase composition due to the presence of carbon and nitrogen in the composite, as indicated by their XRD profiles. Furthermore, the peak at $2\theta = \sim 30.8^{\circ}$ (1 2 1) was eliminated in the bio-inspired TiO_2 hybrid composite due to the fact that C/N prevents the formation of brookite [28]. Carbon and nitrogen spices that have been coated with TiO_2 are also present, probably as a result of the decrease of TiO_2 at the interfaces with surrounding carbon and nitrogen during the annealing process. From the sample's thermogravimetric analysis (TGA), it was possible to measure the amount of C/N present in the bio-inspired TiO_2 hybrid composite (Figure 1(b)). Considering how quickly surface-adsorbed water molecules in the sample may be removed, as well as how rapidly oxidation of TiO_2 can occur at very low temperatures, we hypothesize that the weight change of the sample up to 275°C is caused by both the loss of water and oxidation of TiO_2. Carbon/nitrogen content in the bio-inspired TiO_2 hybrid composite was calculated to be approximately 23.3 weight percent based on this assumption.

The SEM images in Figure 2(a) were taken to examine the surface morphology of the C- and N-doped bio-inspired C/N/TiO_2 hybrid photocatalyst. Figure 2(a) (left) appears to show TiO_2 nanotubes covering the C and N particles. Moreover, the TiO_2 nanotubes are arrayed in a radial pattern, indicating that they are composed of many microscopic C and N nanoparticles, which is consistent with their strong affinity for metal oxide surfaces and ability to generate C and N nanoparticles under controlled conditions of high-temperature sintering. Figure 2(a) (right) shows that the surface of TiO_2 became rougher and that interspace between nanotubes was partially occupied by carbon and nitrogen spices, indicating that carbon and nitrogen doping were successfully functionalized on the TiO_2 nanotube. Furthermore, micropores were observed in Figure 2(a) (right), which generate favorable surface properties to enhance photocatalyst activity over the bio-inspired C/N/TiO_2 hybrid composite under visible light [41]. The specific surface area of bio-inspired C/N/TiO_2 hybrid photocatalyst was 47.8 m^2g^{-1}, while that of doped TiO_2 with carbon and nitrogen was 53 m^2g^{-1}. The slightly enhanced specific surface area of C- and N-doped TiO_2 is, without a doubt, connected to the smaller grain size and the existing pore structure of the material. The enhancement in photocatalytic performance may be attributable to an increase in photocatalytic activity brought about by an increase in specific surface area.

The UV-Vis absorption spectra of a bio-inspired C/N/TiO_2 hybrid composite and pure TiO_2 are shown in Figure 2(b). While pure TiO_2 exhibits absorption exclusively in the ultraviolet range, the complete C- and N-doped bio-inspired C/N/TiO_2 hybrid composite exhibits visible absorption. When C and N are doped into TiO_2, the absorptions of the catalysts are enhanced and stronger in the

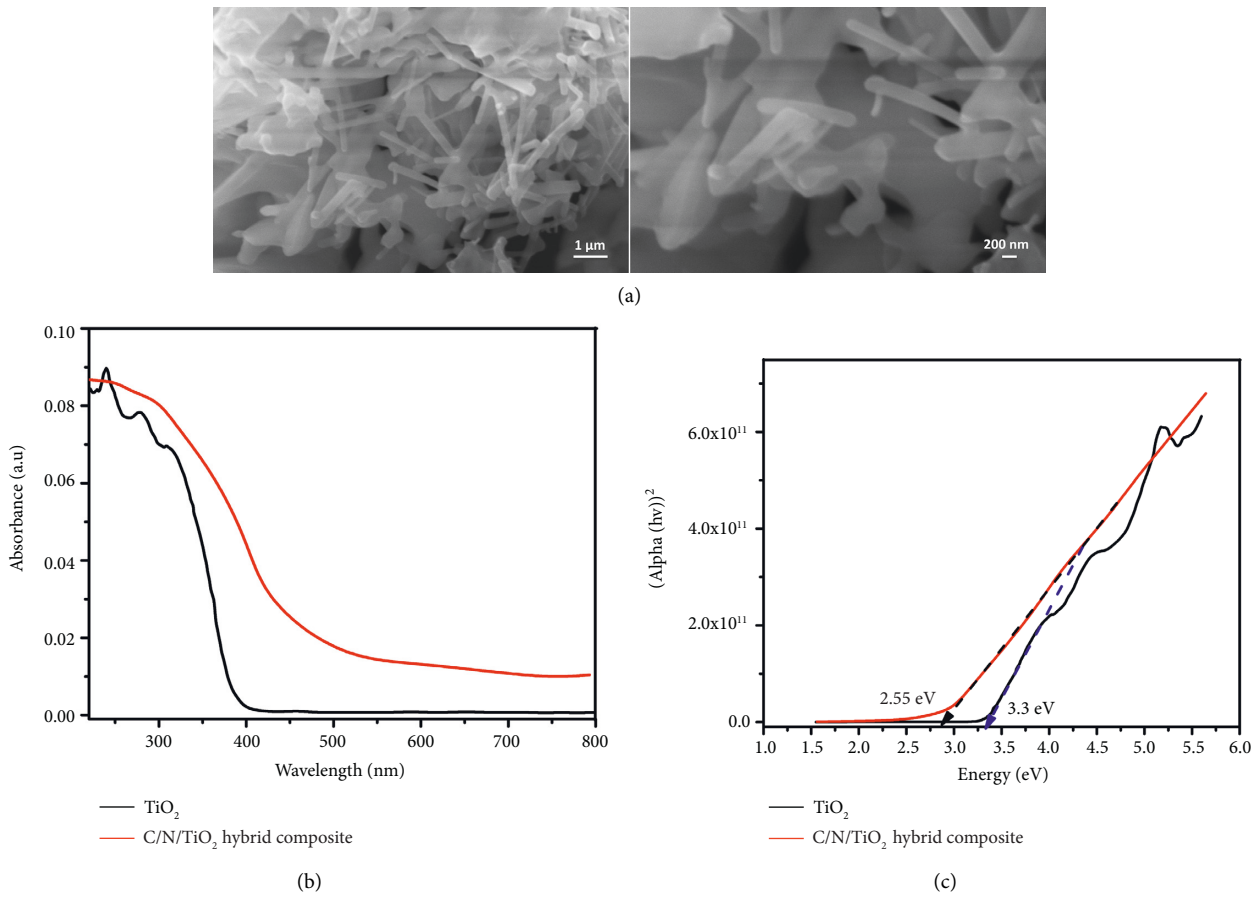

FIGURE 2: (a) SEM images of bio-inspired C/N/TiO_2 hybrid composite. (b) UV-Vis spectra of pure TiO_2 and bio-inspired C/N/TiO_2 hybrid composite. (c) Tauc plots of pure TiO_2 and bio-inspired C/N/TiO_2 hybrid composite.

wavelength range of 400–800 nm incorporation of carbon and nitrogen atoms into the lattice of TiO_2. The photoresponse of C/N/TiO_2 hybrid composite in visible light can be ascribed to the presence of oxygen vacancy states, due to the formation of Ti^{3+} species, between the valence and the conduction bands in the TiO_2 band structure. The vacant oxygen sites may have been substituted by carbon/nitrogen atoms, and these carbon/nitrogen sites are responsible for the visible-light sensitivity. These encouraging results show that adding C and N doping via a bio-inspired method may increase the photocatalytic activity of TiO_2 under visible light. Aside from that, the energy band gaps were computed using the Tauc plots (Figure 2(c)), taking into consideration the absorbance transformed by the Kubelka–Munk function and the band gaps. Furthermore, Tauc plots of bio-inspired C/N/TiO_2 hybrid composite and pure TiO_2 demonstrate (Figure 2(c)) that the energy band gap decreases from TiO_2 (3.3 eV) to C- and N-doped bio-inspired C/N/TiO_2 hybrid composite (2.55 eV), which is less than previously reported carbon- and nitrogen-doped TiO_2 photocatalysts [42–45]. This showed that electrons in the valence band may more easily travel into the conduction band and create electron-hole pairs, which could be advantageous in improving the redox characteristics of the catalysts when exposed to sunlight.

As can be seen in Figure 3(a), the FT-IR spectra of pure TiO_2 and C/N co-doped bio-inspired C/N/TiO_2 hybrid composite both have wavelengths in the 400–4000 cm^{-1} range. The spectra were obtained using different wavelengths of infrared radiation, which revealed the vibrations of different groups of molecules. The usual N-H properties of urea can be observed in Figure 3(a) between 3200–3600 cm^{-1} and 1650–1700 cm^{-1}, as illustrated in Figure 3(a) [46, 47]. In particular, the related O-H stretching modes, which are derived from surface water molecules, are responsible for a prominent peak at 3335 cm^{-1}. It is possible to detect the bending vibration associated with the molecular water bending band at a wavelength of 1680 cm^{-1} as a result of TiO_2 nanoparticle water absorption at this wavelength [48]. The 1350 cm^{-1} band is caused by the in-plane skeletal vibrations of aromatic rings. The broad bands in the region 700 cm^{-1} and 550 cm^{-1} bands were assigned to Ti-O and Ti-O-Ti stretching vibrations of TiO_6 [49]. We believe that the main adsorption peak at 570 cm^{-1} in pure TiO_2 shifted to 650 cm^{-1} in C/N/TiO_2 hybrid composite due to the transformation of brookite to anatase crystal phase, as justified by XRD (Figure 1(a)). Figure 3(b) shows photoluminescence spectra of pure TiO_2 and a bio-inspired C/N/TiO_2 hybrid composite, which were used to explore the recombination of electron-hole pairs on TiO_2 surfaces. When comparing the

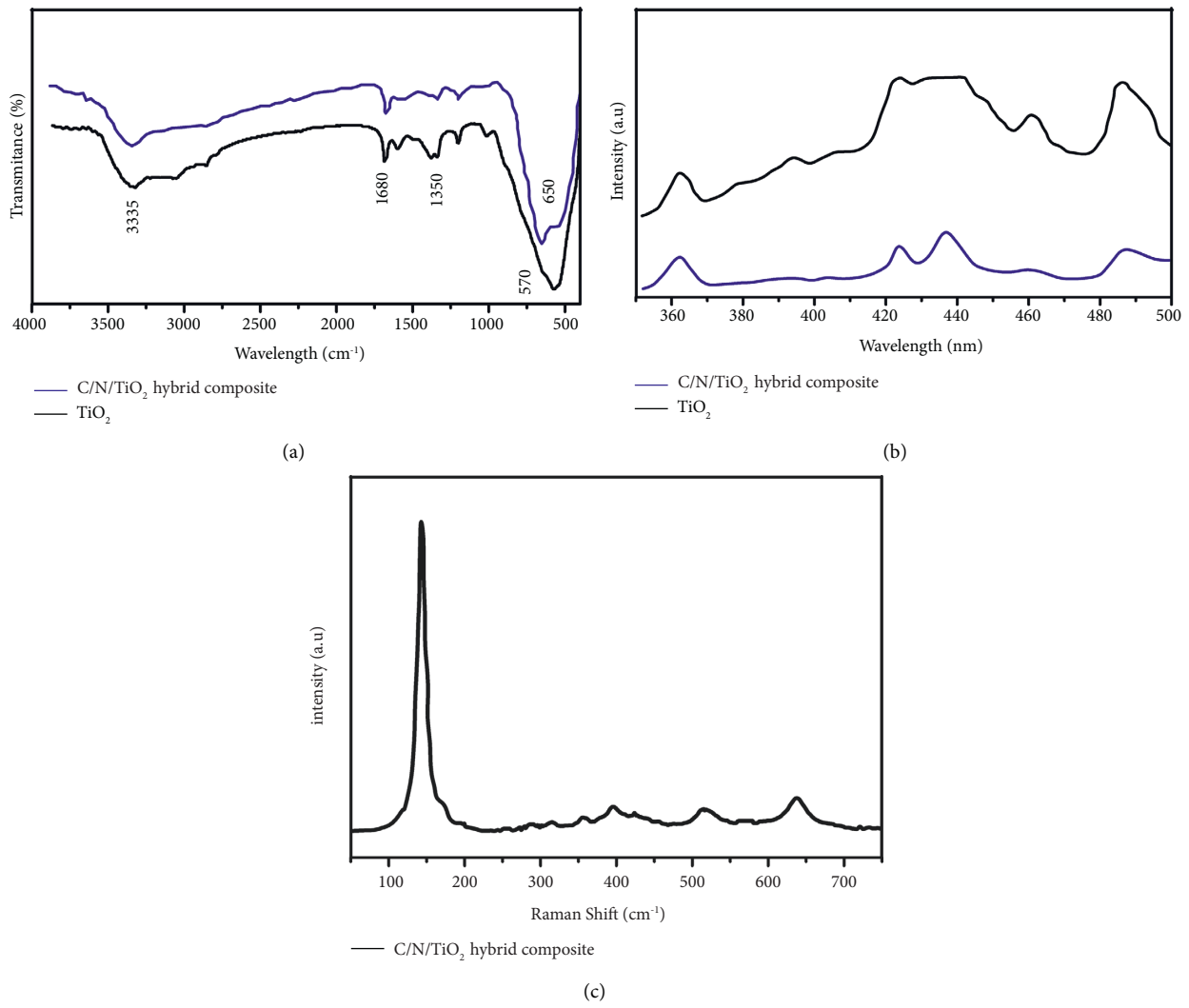

Figure 3: (a) FTIR. (b) Photoluminescence. (c) Raman spectra of pure TiO_2 and bio-inspired C/N/TiO_2 hybrid composite.

luminescence efficiency of the hybrid C/N/TiO_2 and the pure TiO_2, it is found that electron transfer from excited TiO_2 to carbon and nitrogen, which is known to hinder electron recombination, has had a detrimental effect on the composites' ability to recombine electron-hole pairs. This recombination occurs between bands at 364 nm, resulting in the photoluminescence peak at this wavelength (Figure 3(b)). A surface state and defect-related peak may be found in the 400–450 nm range, while a peak in the 460–470 nm range can be attributed to indirect recombination via oxygen defects.

Raman spectroscopy is a technique used to study the vibrational and rotational energy of molecules. When applied to nanomaterials, Raman spectroscopy can be used to gain insight into the crystallinity, composition, and structure of the material. In this study, Raman spectra were collected from a C/N/TiO_2 hybrid composite photocatalyst in order to investigate its activity. Figure 3(c) shows the Raman spectra of C/N/TiO_2 hybrid composite. In particular, the Raman peaks at roughly 144 (E_g), 203 (E_g), 399 ($B1_g$), 519 ($B1_g$), and 639 (E_g) cm^{-1} and the spectral pattern fit well with the results that have been reported in the literature for typical anatase TiO_2 [50, 51]. In addition to this, Figure 3(c) displays an additional feature in the vicinity of 560 cm^{-1} [51]. The XRD patterns and the results of the spectrum show that anatase TiO_2 is the predominant phase in the C/N-doped TiO_2 sample. This finding is consistent with the findings of the spectrum [51]. The first-order scattering produced by a nonstoichiometric nitrogen/carbon-doped anatase TiO_2 structure is responsible for this characteristic's appearance. Therefore, Raman spectra are evidence that the material is a C/N-doped TiO_2 compound.

The photocatalytic activity was observed by the deterioration of RhB in an aqueous solution when exposed to visible light. RhB absorbs the most light at a wavelength of approximately 553 nm. During the photodegradation process, the primary absorption band experienced significant hypsochromic alterations. The absorption peak gradually decreased as the visible light was irradiated, demonstrating the decomposition of the RhB compound in consideration. All rhodamine species were measured using the maximum absorption method, which was used to determine their total

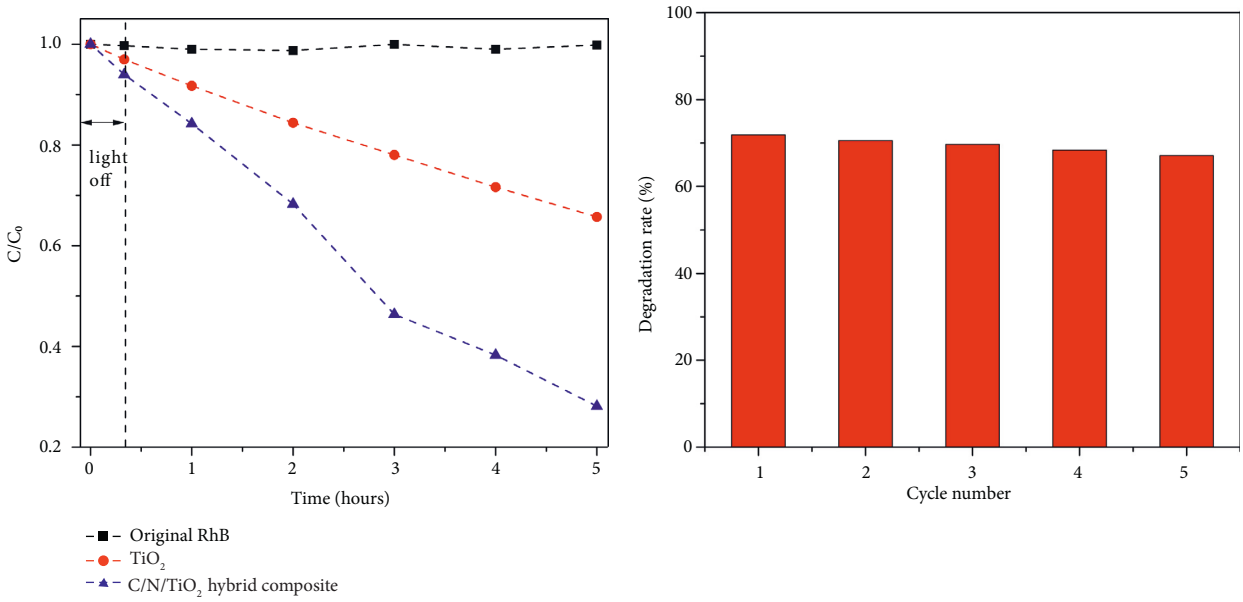

FIGURE 4: (a) Photocatalytic degradation of RhB in the absence of light (upto 20 min) and the presence of pure TiO_2 and bio-inspired C/N/TiO_2 hybrid composite under visible-light irradiation. (b) 5 cycles of degradation of RhB using C/N/TiO_2 hybrid composite as the photocatalyst.

concentrations. Figure 4(a) displays the photodegradation behavior of RhB dye in the absence of any light (dark test), and in the presence of the as-prepared TiO_2, and C/N/TiO_2 hybrids after exposure to visible-light irradiation, where C is the concentration of RhB after different light irradiation times and C_0 is the initial concentration of RhB before dark adsorption. RhB content in aqueous solution decreases when C/N/TiO_2 hybrid composite or pure TiO_2 is present, and RhB self-degrades when exposed to ultraviolet light ($\lambda > 400$ nm) as depicted in Figure 4(a). It was discovered that the self-degradation of RhB was not readily apparent, indicating that RhB has been stabilized by exposure to visible-light irradiation. At 0 hours, in the presence of visible light, RhB deterioration on TiO_2 and C/N/TiO_2 hybrid composites has been observed. This is attributable to the self-sensitization of RhB, which causes the absorption of titania to extend into the visible-light range.

Furthermore, with the presence of as-prepared pure TiO_2 and bio-inspired C/N/TiO_2 hybrid composite photocatalysts, the degradation of RhB is observed as 9 and 16 percent after one hour and 35 and 70 percent after five hours under sunlight, respectively. RhB was used as a sensitizer in this instance, but it was also degraded at the same time. On the degradation of RhB, it was clear that the photocatalytic activity of the C/N/TiO_2 hybrid composite outperformed that of as-prepared pure TiO_2 as generated by the bio-inspired route. Even more importantly, the bio-inspired C/N/TiO_2 hybrid composite photocatalyst demonstrated significantly greater photocatalytic activity on the degradation of RhB when exposed to visible-light irradiation than commercial TiO_2 and P25 because of the lowered energy bandgap.

There are three possible explanations for the strong visible-light activity of the hybrid composite of C/N-doped TiO_2. First, C/N-doped TiO_2 with a high surface area is able to supply more active sites and absorb more reactive species, which may have been the explanation for its increased photocatalytic activity. TiO_2 has a high atomic number. Because the TiO_2 had already been created prior to the doping process, it is believed that the carbon and nitrogen may be able to replace for some of the lattice titanium atoms that are close to or on the surface of the TiO_2. As a result, a narrowing of the band gap occurred in the C/N/TiO_2 hybrid composite, which enabled it to absorb more visible light. Because the surface lattice titanium atoms of the TiO_2 sample had a certain amount, which resulted in a limited accommodation for carbon and nitrogen substitutions, these substitutions of surface lattice titanium atoms may explain why doped TiO_2 catalysts with different doping amounts of carbon and nitrogen showed similar photocatalytic activities. The reduction of urea and tannic acid during the hydrothermal process is thought to have resulted in the incorporation of carbonaceous and nitrogen species into the TiO_2 matrix, as the final hypothesis suggests. It is possible that this will result in the development of new active sites, which are also accountable for the increased photocatalytic activity that was observed. Figure 4(b) depicts the photodegradation of RhB over five cycles. As shown in Figure 4(b), after 5 cycles of photodegradation of RhB, the photocatalytic activity of the CNT/TiO_2 nanohybrids shows a slight decrease due to partial remembrance and loss during washing. Despite the fact that the photocatalytic activity was initially quite high, this is the case. As a result, the photocatalyst C/N/TiO_2 nanohybrids developed are quite stable and have a significant amount of potential application in the field of water purification.

The photocatalytic mechanism of bio-inspired C/N/TiO_2 hybrid composite heterostructure is a result of the combined

effects of the light-induced charge separation at the semiconductor/oxide interface and the electron-transfer reactions between the catalyst and the substrate. In addition, photogenerated electrons and holes can be absorbed by adsorbed oxygen molecules and surface hydroxyl, respectively, both of which result in the creation of highly oxidative hydroxyl radical species (•OH) [12]. Because of their great oxidative capacity, (•OH) molecules attack dye molecules with minimal selectivity and are able to oxidize contaminants because of their high oxidative potential. Additionally, the bio-inspired C/N/TiO_2 hybrid composite heterostructure has a higher surface area and improved interfacial contact, which enhances the photocatalytic activity.

Our findings give evidence that the carbon in C/N-TiO_2 can facilitate its photocatalytic activity under visible light by maintaining the high reactivity of the photogenerated electrons and holes. This is demonstrated by the fact that the photocatalytic activity is enhanced. A novel precursor approach to manufacture C/N-doped TiO_2 modified by C components with high nitrogen concentration has been developed as a result of this investigation. It is hoped that the bioinspired hydrothermal precursor approach would throw light on the creation of doping materials that have been changed with carbon and nitrogen, with the end goal of increasing the visible-light photocatalytic activity of TiO_2. We believe that the presence of nitrogen in the structure allows for more efficient electron transfer from the excited titanium dioxide to the organic molecule, resulting in a higher photocatalytic activity. Additionally, the bio-inspired structure may provide a more favorable surface area for light absorption and catalyst activation. Thus, it demonstrates the bio-inspired carbon- and nitrogen-doped C/N/TiO_2 hybrid composite is an excellent visible-light-driven photocatalyst.

4. Conclusions

With the use of a unique bio-inspired technique and carbon and nitrogen doping at 500 degrees Celsius, a visible-light-active C/N/TiO_2 hybrid photocatalyst composite was successfully synthesized by the hydrothermal method. When compared to P25 and pure TiO_2, carbon- and nitrogen-modified TiO_2 had a higher surface area and displayed more absorption in the visible-light range. It was discovered that carbon/nitrogen-doped TiO_2 prepared by treating it with tannic acid and urea had considerably better photocatalytic activity than pure TiO_2 when exposed to visible light ($\lambda > 400$ nm) for the degradation of RhB. Because of its simplicity, ecological, and sustainable energy-saving characteristics, this approach has the potential to be used in the industrial manufacture of visible-light-driven photocatalysts in the future.

Data Availability

All data have been included within the article.

Conflicts of Interest

The authors declare that they have no conflicts of interest.

References

[1] J. J. Rueda-Marquez, I. Levchuk, P. Fernández Ibañez, and M. Sillanpää, "A critical review on application of photocatalysis for toxicity reduction of real wastewaters," *Journal of Cleaner Production*, vol. 258, Article ID 120694, 2020.

[2] W.-K. Jo and R. J. Tayade, "New generation energy-efficient light source for photocatalysis: LEDs for environmental applications," *Industrial & Engineering Chemistry Research*, vol. 53, no. 6, pp. 2073–2084, 2014.

[3] R. Ahmad, Z. Ahmad, A. U. Khan, N. R. Mastoi, M. Aslam, and J. Kim, "Photocatalytic systems as an advanced environmental remediation: recent developments, limitations and new avenues for applications," *Journal of Environmental Chemical Engineering*, vol. 4, pp. 4143–4164, 2016.

[4] N. R. Lakkimsetty, S. Feroz, S. Karunya, L. Motilal, P. Saidireddy, and G. Suman, "Synthesis, characterization and application of polymer composite materials in wastewater treatment," *Materials Today Proceedings*, vol. 59, pp. 1726–1734, 2022.

[5] N. R. Lakkimsetty, M. Lakavat, M. Varghese, and S. Gandi, "Solar photo catalytic treatment of oil produced water using zinc oxide," *AIP Conference Proceedings*, vol. 2396, Article ID 020010, 2021.

[6] M. Al-Balushi, N. R. Lakkimsetty, M. Varghese, M. Lakavat, P. S. Reddy, and S. Gandi, "Evaluating the solar photo-fenton as photocatalyst process by response surface methodology to treat the saline water," *Materials Today Proceedings*, 2021.

[7] K. Hashimoto, H. Irie, and A. Fujishima, "TiO_2Photocatalysis: a historical overview and future prospects," *Japanese Journal of Applied Physics*, vol. 44, no. 12, pp. 8269–8285, 2005.

[8] Q. Guo, Z. Ma, C. Zhou, Z. Ren, and X. Yang, "Single molecule photocatalysis on TiO_2 surfaces," *Chemical Reviews*, vol. 119, no. 20, pp. 11020–11041, 2019.

[9] S. Leong, A. Razmjou, K. Wang, K. Hapgood, X. Zhang, and H. Wang, "TiO_2 based photocatalytic membranes: a review," *Journal of Membrane Science*, vol. 472, pp. 167–184, 2014.

[10] M. Al-Mamun, S. Kader, M. Islam, and M. Khan, "Photocatalytic activity improvement and application of UV-TiO_2 photocatalysis in textile wastewater treatment: a review," *Journal of Environmental Chemical Engineering*, vol. 7, no. 5, Article ID 103248, 2019.

[11] D. Chen, Y. Cheng, N. Zhou et al., "Photocatalytic degradation of organic pollutants using TiO_2-based photocatalysts: a review," *Journal of Cleaner Production*, vol. 268, Article ID 121725, 2020.

[12] S. Du, J. Lian, and F. Zhang, "Visible light-responsive N-doped TiO_2 photocatalysis: synthesis, characterizations, and applications," *Transactions of Tianjin University*, vol. 28, no. 1, pp. 33–52, 2022.

[13] S. Zheng, W. Jiang, Y. Cai, D. D. Dionysiou, and K. E. O'Shea, "Adsorption and photocatalytic degradation of aromatic organoarsenic compounds in TiO_2 suspension," *Catalysis Today*, vol. 224, pp. 83–88, 2014.

[14] S. R. Pouran, A. Bayrami, A. A. Aziz, W. M. A. W. Daud, and M. S. Shafeeyan, "Ultrasound and UV assisted fenton treatment of recalcitrant wastewaters using transition metal-substituted-magnetite nanoparticles," *Journal of Molecular Liquids*, vol. 222, p. 1076, 2016.

[15] H. Dong, G. Zeng, L. Tang et al., "An overview on limitations of TiO_2-based particles for photocatalytic degradation of organic pollutants and the corresponding countermeasures," *Water Research*, vol. 79, pp. 128–146, 2015.

[16] M. Nasr, C. Eid, R. Habchi, P. Miele, and M. Bechelany, "Recent progress on titanium dioxide nanomaterials for photocatalytic applications," *ChemSusChem*, vol. 11, no. 18, pp. 3023–3047, 2018.

[17] M. Pelaez, N. T. Nolan, S. C. Pillai et al., "A review on the visible light active titanium dioxide photocatalysts for environmental applications," *Applied Catalysis B: Environmental*, vol. 125, pp. 331–349, 2012.

[18] M. Humayun, F. Raziq, A. Khan, and W. Luo, "Modification strategies of TiO_2 for potential applications in photocatalysis: a critical review," *Green Chemistry Letters and Reviews*, vol. 11, no. 2, pp. 86–102, 2018.

[19] M. Nasirian, Y. P. Lin, C. F. Bustillo-Lecompte, and M. Mehrvar, "Enhancement of photocatalytic activity of titanium dioxide using non-metal doping methods under visible light: a review," *International Journal of Environmental Science and Technology*, vol. 15, no. 9, pp. 2009–2032, 2018.

[20] P. S. Basavarajappa, S. B. Patil, N. Ganganagappa, K. R. Reddy, A. V. Raghu, and C. V. Reddy, "Recent progress in metal-doped TiO_2, non-metal doped/codoped TiO_2 and TiO_2 nanostructured hybrids for enhanced photocatalysis," *International Journal of Hydrogen Energy*, vol. 45, no. 13, pp. 7764–7778, 2020.

[21] A. K. R. Police, S. P. Vattikuti, Y.-J. Baik, and B. Chan, "Eco-friendly, hydrogen fluoride-free, morphology-oriented synthesis of TiO_2 with exposed (001) facets," *Ceramics International*, vol. 45, no. 2, pp. 2178–2184, 2019.

[22] R. Qian, H. Zong, J. Schneider et al., "Charge carrier trapping, recombination and transfer during TiO_2 photocatalysis: an overview," *Catalysis Today*, vol. 335, pp. 78–90, 2019.

[23] J. P. Jeon, D. H. Kweon, B. J. Jang, M. J. Ju, and J. B. Baek, "Enhancing the photocatalytic activity of TiO_2 catalysts," *Advanced Sustainable Systems*, vol. 4, no. 12, Article ID 2000197, 2020.

[24] L. Zhou, H. Zhang, H. Sun et al., "Recent advances in non-metal modification of graphitic carbon nitride for photocatalysis: a historic review," *Catalysis Science and Technology*, vol. 6, no. 19, pp. 7002–7023, 2016.

[25] S. Rehman, R. Ullah, A. Butt, and N. Gohar, "Strategies of making TiO_2 and ZnO visible light active," *Journal of Hazardous Materials*, vol. 170, no. 2-3, pp. 560–569, 2009.

[26] Y. Yalcin, M. Kilic, and Z. Cinar, "The role of non-metal doping in TiO_2 photocatalysis," *Journal of Advanced Oxidation Technologies*, vol. 13, p. 281, 2010.

[27] T. C. Jagadale, S. P. Takale, R. S. Sonawane et al., "N-doped TiO_2 nanoparticle based visible light photocatalyst by modified peroxide sol-gel method," *Journal of Physical Chemistry C*, vol. 112, no. 37, pp. 14595–14602, 2008.

[28] C. Sushma and S. G. Kumar, "C-N-S tridoping into TiO_2 matrix for photocatalytic applications: observations, speculations and contradictions in the codoping process," *Inorganic Chemistry Frontiers*, vol. 4, no. 8, pp. 1250–1267, 2017.

[29] Q. Chen, A. Ozkan, B. Chattopadhyay et al., "N-doped TiO_2 photocatalyst coatings synthesized by a cold atmospheric plasma," *Langmuir*, vol. 35, no. 22, pp. 7161–7168, 2019.

[30] S. V. P. Vattikuti, K. C. Devarayapalli, N. K. Reddy Nallabala, T. N. Nguyen, N. Nguyen Dang, and J. Shim, "Onion-Ring-like carbon and nitrogen from ZIF-8 on TiO_2/Fe_2O_3 nanostructure for overall electrochemical water splitting," *Journal of Physical Chemistry Letters*, vol. 12, no. 25, pp. 5909–5918, 2021.

[31] A. S. Nur, M. Sultana, A. Mondal et al., "A review on the development of elemental and codoped TiO_2 photocatalysts for enhanced dye degradation under UV-vis irradiation," *Journal of Water Process Engineering*, vol. 47, Article ID 102728, 2022.

[32] V. Hasija, P. Raizada, A. Sudhaik et al., "Recent advances in noble metal free doped graphitic carbon nitride based nanohybrids for photocatalysis of organic contaminants in water: a review," *Applied Materials Today*, vol. 15, pp. 494–524, 2019.

[33] K. Lee, H. Yoon, C. Ahn, J. Park, and S. Jeon, "Strategies to improve the photocatalytic activity of TiO_2: 3D nanostructuring and heterostructuring with graphitic carbon nanomaterials," *Nanoscale*, vol. 11, no. 15, pp. 7025–7040, 2019.

[34] J. Tian, Y. Leng, Z. Zhao et al., "Carbon quantum dots/hydrogenated TiO_2 nanobelt heterostructures and their broad spectrum photocatalytic properties under UV, visible, and near-infrared irradiation," *Nano Energy*, vol. 11, pp. 419–427, 2015.

[35] M. Peñas-Garzón, A. Gómez-Avilés, C. Belver, J. Rodriguez, and J. Bedia, "Degradation pathways of emerging contaminants using TiO_2-activated carbon heterostructures in aqueous solution under simulated solar light," *Chemical Engineering Journal*, vol. 392, Article ID 124867, 2020.

[36] M. A. Mohamed, W. N. W. Salleh, J. Jaafar et al., "Carbon as amorphous shell and interstitial dopant in mesoporous rutile TiO_2: bio-template assisted sol-gel synthesis and photocatalytic activity," *Applied Surface Science*, vol. 393, p. 46, 2017.

[37] M. A. Mohamed, N. A. Rahman, M. Zain et al., "Hematite microcube decorated TiO_2 nanorods as heterojunction photocatalyst with in-situ carbon doping derived from polysaccharides bio-templates hydrothermal carbonization," *Journal of Alloys and Compounds*, vol. 820, Article ID 153143, 2020.

[38] A. Kumar, G. Sharma, M. Naushad et al., "Bio-inspired and biomaterials-based hybrid photocatalysts for environmental detoxification: a review," *Chemical Engineering Journal*, vol. 382, Article ID 122937, 2020.

[39] Y. Xiang, W. Zhu, W. Guo et al., "Controlled carbon coating of Fe_2O_3 nanotube with tannic acid: a bio-inspired approach toward high performance lithium-ion battery anode," *Journal of Alloys and Compounds*, vol. 719, pp. 347–352, 2017.

[40] W. Ren, Z. Ai, F. Jia, L. Zhang, X. Fan, and Z. Zou, "Low temperature preparation and visible light photocatalytic activity of mesoporous carbon-doped crystalline TiO_2," *Applied Catalysis B: Environmental*, vol. 69, no. 3-4, pp. 138–144, 2007.

[41] H.-B. Huang, Y. Wang, F.-Y. Cai et al., "Photodegradation of rhodamine B over biomass-derived activated carbon supported CdS nanomaterials under visible irradiation," *Frontiers of Chemistry*, vol. 5, p. 123, 2017.

[42] D. Wu, M. Long, W. Cai, C. Chen, and Y. Wu, "Low temperature hydrothermal synthesis of *N*-doped TiO_2 photocatalyst with high visible-light activity," *Journal of Alloys and Compounds*, vol. 502, no. 2, pp. 289–294, 2010.

[43] S. Sharma, S. Kumar, S. M. Arumugam, and S. Elumalai, "Promising photocatalytic degradation of lignin over carbon quantum dots decorated TiO_2 nanocomposite in aqueous condition," *Applied Catalysis A: General*, vol. 602, Article ID 117730, 2020.

[44] N. C. Martins, J. Ângelo, A. V. Girão, T. Trindade, L. Andrade, and A. Mendes, "*N*-doped carbon quantum dots/TiO_2 composite with improved photocatalytic activity," *Applied Catalysis B: Environmental*, vol. 193, pp. 67–74, 2016.

[45] L. N. Quan, Y. H. Jang, K. A. Stoerzinger et al., "Soft-template-carbonization route to highly textured mesoporous carbon-TiO_2 inverse opals for efficient photocatalytic and

photoelectrochemical applications," *Physical Chemistry Chemical Physics*, vol. 16, no. 19, pp. 9023–9030, 2014.

[46] M. Azami, W. Nawawi, A. H. Jawad, M. Ishak, and K. Ismail, "*N*-doped TiO_2 synthesised via microwave induced photocatalytic on RR4 dye removal under LED light irradiation," *Sains Malaysiana*, vol. 46, no. 8, pp. 1309–1316, 2017.

[47] M. A. Larrubia, G. Ramis, and G. Busca, "An FT-IR study of the adsorption of urea and ammonia over V_2O_5–MoO_3–TiO_2 SCR catalysts," *Applied Catalysis B: Environmental*, vol. 27, no. 3, pp. L145–L151, 2000.

[48] K. Nagaveni, G. Sivalingam, M. Hegde, and G. Madras, "Solar photocatalytic degradation of dyes: high activity of combustion synthesized nano TiO_2," *Applied Catalysis B: Environmental*, vol. 48, no. 2, pp. 83–93, 2004.

[49] A. K. Rai, K. Rao, L. V. Kumar, and K. Mandal, "Synthesis and characterization of ultra fine barium calcium titanate, barium strontium titanate and Ba1–2xCaxSrxTiO$_3$ (x = 0.05, 0.10)," *Journal of Alloys and Compounds*, vol. 475, p. 316, 2009.

[50] N. T. Lan, V. H. Anh, H. D. An et al., "Synthesis of C-N-S-tridoped TiO_2 from vietnam ilmenite ore and its visible light-driven-photocatalytic activity for tetracyline degradation," *Journal of Nanomaterials*, vol. 2020, Article ID 1523164, 14 pages, 2020.

[51] A. M. Abdullah, N. J. Al-Thani, K. Tawbi, and H. Al-Kandari, "Carbon/nitrogen-doped TiO_2: new synthesis route, characterization and application for phenol degradation," *Arabian Journal of Chemistry*, vol. 9, no. 2, pp. 229–237, 2016.